Int J Adv Manuf Technol (2001) 18:348–356

The International Journal of
Advanced
Manufacturing
Technology

An Investigation of Wax Patterns for Accuracy Improvement in Investment Cast Parts

W. Bonilla, S. H. Masood and P. Iovenitti

Industrial Research Institute Swinburne, Swinburne University of Technology, Hawthorn, Melbourne, Australia

In this paper, a methodology is proposed that makes use of computer-aided heat transfer simulation and experimentally derived factors for injection parameters, to predict wax pattern shrinkages in the investment casting process. The focus is on developing techniques for the early determination of optimum injection parameters to be used for wax pattern production so that resulting shrinkage can translate into an overall improvement in accuracy of the investment casting process.

Keywords: Injection parameters; Investment casting; Shrinkage; Simulation; Wax pattern

1. Introduction

Investment casting is sometimes referred to as a near net shape casting process and it is often preferred to other casting processes because of its many advantages. Application to parts with intricate geometry combined with high accuracy, and the relative ease of producing components with internal cavities, good surface finish, and good castability with a large variety of alloys [1,2] are some of the advantages which justify its preference to other processes.

The investment casting process consists of a number of smaller processes, each of which has its own complexities. There are three major stages in investment casting: the production of wax patterns, the production of the ceramic moulds and the metal casting itself. At each of these stages there are dimensional changes. These have to be accounted for by applying shrinkage allowances so that the required final dimensions of the cast part can be achieved as accurately as possible.

As the demand for tighter tolerances from investment casting grows, it becomes economically and competitively important for the investment caster to be able to have the best possible control of the factors that affect the accuracy of the final cast component. This is particularly so in the case of large orders of high-tolerance components.

The accuracy of the wax patterns used in the investment casting process has a direct bearing on the accuracy achievable in the final cast part. It is usual for the investment caster to use precision-machined full-metal dies for producing wax patterns when large numbers of highly accurate components are required [3]. A die of this kind can be costly, and there is usually a considerable lead time associated with its production. In deciding the dimensions of the die cavity to be machined, there are two main shrinkage allowances to be considered: the die-to-wax shrinkage and the casting solidification shrinkage. If these allowances are not correct and the final cast–part tolerances are not met, then extra costs and time are incurred because the tooling must be reworked. It is, therefore, very important to ensure that all the appropriate factors are considered when applying the shrinkage allowances.

Considering the accuracy of the wax pattern production process, it is found that a number of factors affect the amount of dimensional contraction in wax patterns made from the die. It has been reported [4] that the injection parameters play an important role in the accuracy of the wax patterns. These parameters include: the injection flowrate; the injection cycle time; the injection temperature; the injection pressure; and the die temperature. Some of the effects of these parameters on wax pattern accuracy are known. It is reported that contraction decreases when cycle time and/or the injection pressure are increased. Injection flowrate appears to have a smaller effect on wax pattern dimensions.

It appears that there is no consistency in the way investment casters decide on the application of their tooling shrinkage allowances, nor are there any guidelines available to the industry in deciding appropriate values of such allowances. Okhuysen et al. [5] reported the results of a survey of 18 investment casting companies to determine the tooling allowance practices. They found great variations in the tooling allowances used from one investment casting company to another ranging from 1.2% to 3.8% even though all results were collected for casting the same alloys. They used correction factors for different pattern materials.

This paper presents the results of on-going work being carried out at the Industrial Research Institute Swinburne (IRIS)

Correspondence and offprint requests to: Dr S. H. Masood, Associate Professor, Industrial Research Institute Swinburne, Swinburne University of Technology, Hawthorn, Melbourne 3122, Australia. E-mail: smasood@swin.edu.au

on accuracy improvement of investment cast parts. A computer-based methodology involving heat transfer simulation and contraction of solids is used to determine the final contraction in wax patterns. The results also include an experimental investigation of the effect of injection parameters on the dimensional accuracy of the wax pattern.

2. Modelling the Wax Pattern Contraction Process

Because of the change in temperature occurring in the pattern material as it cools from injection temperature to room temperature there is an associated change in volume that can be accurately predicted if the material properties are known. However, there are a large number of factors such as injection parameters, die cooling regime, part size and geometry, which affect the degree of the changes in this ideal behaviour of the material.

Modelling of the contraction process, as proposed here, is undertaken by combining the physics of solid contraction and heat transfer with the experimentally derived factors that affect injection parameters.

2.1 Theory of Expansion and Contraction of Solids

Most solids, including pattern materials, expand when heated, and contract when cooled. The magnitude of the dimensional changes is directly dependent on the magnitude of the temperature change. The change in volume owing to a temperature difference can ideally be described by the well-known relationship shown in Eq. (1).

$$\Delta V = \beta\ V_i\ (T_i - T_f) \tag{1}$$

where,

ΔV = change in volume
β = volumetric coefficient of thermal expansion
V_i = initial volume
T_i = initial temperature
T_f = final temperature

This ideal contraction can also be modelled graphically in a CAD system. For example, in the Pro/MECHANICA-THERMAL module of the Pro/ENGINEER CAD system, a temperature distribution can be obtained after running a heat transfer analysis. This temperature distribution is then applied to the model in the Pro/MECHANICA-STRUCTURE module and the changes in dimension can be simulated. Pro/MECHANICA-THERMAL and -STRUCTURE are advanced modules of the Pro/ENGINEER CAD system. They are used to analyse heat transfer, stresses, strains, deformations, and vibration problems.

The changes in temperature in the case of the wax pattern injection process come about through the heat transfer that occurs, first, when the pattern cools in the die, and, secondly, when the pattern is ejected and cools down to room temperature.

2.2 Theory of Heat Transfer

The defining equation for thermal conductivity, k, of a material is shown in Eq. (2), in which q is the heat transfer rate and A is the area normal to heat flow. The one-dimensional heat conduction equation is shown in Eq. (3). In order to calculate the one-dimensional transient heat transfer, Eq. (2) is used and the temperature gradient is obtained from Eq. (3).

$$q = kA\ \frac{\partial T}{\partial x}, \text{ where, } \frac{\partial T}{\partial x} \text{ is the temperature gradient} \tag{2}$$

$$\frac{\partial^2 T}{\partial^2 x} = \frac{1}{\alpha}\ \frac{\partial T}{\partial z} \tag{3}$$

In practice, an analytical method for evaluating the heat transfer occurring in wax pattern injection is nearly impossible. However, an analytical solution exists for a simplified case of 1D conduction, as is approximately the case for the test component used in the experiments described later in this paper. For a flat plate in 1D conduction the temperature distribution is described by the Fourier series formula shown in Eq. (4), where the variables are described by analogy to a pattern cooling inside a die cavity. Therefore the heat loss for a particular cooling time, or the time needed to reach a particular temperature, while the pattern cools inside the die, can be computed. This can be fed back into Eq. (1) to calculate the ideal in-die contraction.

$$\frac{t - t_1}{t_i - t_1} = \left\{ \frac{4}{\pi} \sum_{n=0}^{\infty} \frac{1}{2n+1} \exp\left(-\left[(2n+1)\ \frac{\pi}{2L}\right]^2 \alpha\tau\right) \sin\left[\frac{(2n+1)\ \pi\ x}{2L}\right] \right\} \tag{4}$$

t = temperature at any time and location
t_1 = temperature of the die cavity wall
t_i = injection temperature
x = position accross the pattern thickness (0 to $2L$)
L = half the thickness of the pattern
τ = time variable, used for cycle time
α = thermal diffussivity of the pattern material

The formulae for the calculation of heat transfer, for the case when the part has been ejected from the die, are also readily available for this simplified case. Therefore, after the ideal in-die contraction, an ideal after-ejection contraction can also be calculated to arrive at the total ideal contraction. Once the ideal contraction has been calculated, the experimentally derived factors affecting injection parameters can be superimposed on top of the initial model to arrive at a model which more closely approximates to the actual behaviour.

3. Heat Transfer Simulation

The heat transfer simulations can be carried out with the aim of establishing and validating a methodology to model the contraction process initially using a simplified case corresponding to the experimental trials. Once the initial case has been validated, advantage can be taken of the existing computer

Table 1. Die and pattern materials properties used for numerical simulation.

Material	AL5083	SI units	Pattern	SI units
Conductivity	k_1	117.61	k2	0.27
Specific heat	c_1	962.3	c2	3343
Density	d_1	2660	d2	969
Initial temperature	ti_1	18	ti2	60
Diffusivity	alf_1	4.59×10^5	alf2	8.33×10^8
Element width	dx_1	0.003031	dx2	0.000129
Time step (0.15)	dt_1	0.1	dt2	0.1
Convergence	>=2 criteria	2		2

Holman [6] p. 170, 1D conduction.
Using finite difference for one-dimensional conduction.
From Holman, p. 170 for convergence:
$\frac{(\Delta x)^2}{\alpha \Delta \tau} \geq 2$ i.e. The value of the reciprocal of the fourier number should be less or equal to 2

power available with the current state of technology, to model any other complex part.

The heat transfer simulation is carried out in two ways. In one method, the simulation study is carried out using the Pro/MECHANICA-THERMAL module of the Pro/ENGINEER CAD system. The other method involves setting up an explicit 1D conduction finite-difference scheme for the transient conduction from the pattern for the case when it cools in the die and for the case when cooling occurs after ejection from the die.

To simplify the heat transfer simulation, it is assumed that the wax pattern has a uniform temperature distribution at a time soon after the filling of the die cavity, neglecting the heat dissipation and convection effects during filling. The geometry and size of the plate used in the experimental tests were chosen to approximate to this simplified case based on pre-experimental trials. A more rigorous treatment would involve the analysis of the filling phase. This would require the knowledge of the rheological properties of the wax and the use of injection simulation software such as Moldflow.

The geometry used for the Pro/Engineer simulation is exact, as solid models are used. For the numerical technique, only thicknesses are used, which are 20 mm for the pattern and 38 mm for each die-half, since the simulation is 1D. Table 1 shows the thermal properties of the die material (AL5083) and the pattern material in SI units. These were used as the input for the simulation study. The die was machined out of a commercial aluminium grade AL5083 H112, for which the properties were obtained from the available literature. For the pattern material, which is a water emulsified wax type A7-TC2/E, the material properties were obtained by testing samples. The specific heat was tested on a Perkin Elmer DSC7 differential scanning calorimeter (DSC) and the thermal conductivity was measured on a TC2000 machine. The mean thermal conductivity found for this wax was 0.27 ($W\,m^{-1}.C^{-1}$) and the mean specific heat found was 3343 ($J\,kg^{-1}.C^{-1}$). Figure 1 shows the results of the specific heat test, from which a graph of fraction solidified vs. temperature function can be derived, using the "s"-shaped cumulative area line. This is elaborated in Section 6. The die was mounted on a vertical-clamping horizontal injection press with temperature-controlled platens.

3.1 Simulations Using Pro/THERMAL System

The Pro/MECHANICA-THERMAL module of the Pro/Engineer CAD package was used to simulate the worst-case scenarios of the heat transfers occurring with the experimental model, and to obtain transient and steady-state 3D temperature distributions. These simulations have assisted in the validation of the simplified model used in the numerical simulations. Figure 2 shows the steady-state temperature distribution results of one of the worst-case scenario simulations. A constant temperature of 60°C was applied to the die cavity wall, corresponding to the simulated injection temperature, and

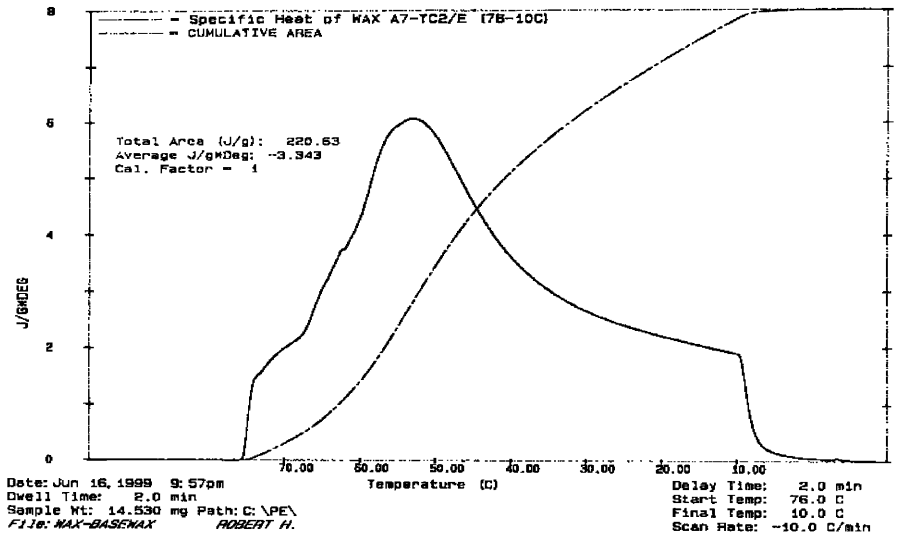

Fig. 1. DSC specific heat trace for wax A7–TC2/E.

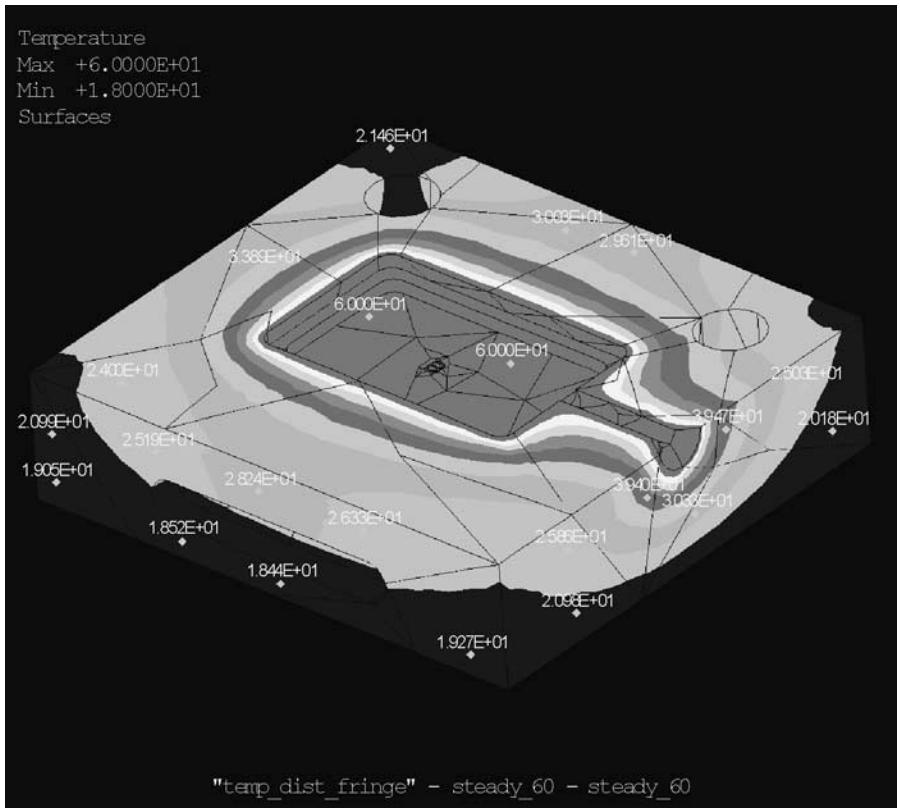

Fig. 2. Temperature distribution of die cavity for worst case scenario.

18°C was applied to the platen face. To simulate convection on the faces exposed to ambient temperature, a convection coefficient of 10 $W\,m^{-1}.C^{-1}$ was used with an ambient temperature of 22°C. The value used for ambient temperature was based on actual wax-room temperatures recorded during the experimental work.

Figure 2 also shows that the maximum temperature gradients are in a direction normal to the platens, which justifies the 1D treatment in this case. It can also be seen that the temperatures on the die faces exposed to air are close to ambient temperature, which means that convection effects during the cycle time can be neglected. These results reinforce the assumptions made and the simplification used in treating the die-system as a 1D heat-conduction problem for this particular case.

3.2 Heat Transfer Simulations by Numerical Technique

To compare numerical results with experimental results, 1D heat-conduction simulations were carried out using an explicit numerical technique from Holman [6]. The transient heat conduction from the injected patterns into the die system is simulated. Figure 3 shows the temperature distribution results of one simulation for an injection temperature of 60°C and a platen temperature of 18°C. This figure shows the simulated temperature distribution across the thickness of the pattern for six different cycle times, which are 1, 2, 3, 4, 5 and 10 min. The right and left sections of Fig. 3 represent the interface of

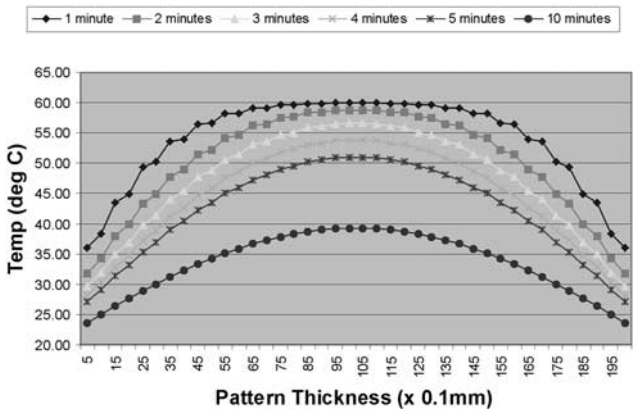

Fig. 3. Pattern thickness temperature distribution by numerical simulation.

the pattern with the die cavity wall. This simulation has not considered thermal contact resistance at the die–platen and die–pattern interfaces and therefore the actual temperature drop with time would be expected to be somewhat slower. However, a useful feature of this graph is for observing the temperature at a depth in the range 4–5 mm from the die wall. It is found that this temperature for the 2, 3, and 4-min cycles ranges between 45°C and 50°C. Compared to the experimental observation of patterns just ejected, which were cut open and the soft material removed and consistently a shell of about 5 mm thickness remained (see Fig. 6), then this temperature represents

the effective minimum ejection temperature for the given pattern material. A practical application of this type of analysis is to consider using it in predicting the required cycle time given a particular component thickness, pattern material, and cooling regime.

4. Experimental Investigations

Figure 4 shows the test pattern used in this investigation. It is a rectangular plate with 5 mm corner radii, with overall dimensions of 104.64 mm long, 64.64 mm wide and 20 mm thick. Rectangular recesses of 5 mm depth were built into the geometry to serve as the surfaces for measurement, with the die parting line at midthickness, which divides the cavity into two symmetrical halves. The injection point is located at one of the 104.64 mm ends and each cavity half is centred on the parting face.

A die of appropriate geometry and size for simplified modelling was machined in Al 5083 H112 to produce wax patterns at different settings of injection parameters. Each die half was fitted with three K-type thermocouples to record cyclic temperature profiles. Only cycle time, injection temperature, and injection pressure were used as variables, as they have been identified as the most important injection parameters affecting pattern accuracy. The following values of injection parameters were used in this investigation:

Injection temperature: 60, 61, 62°C
Injection pressure: 0.74, 0.98, 1.23, 1.48, 1.73, 1.98 MPa
Cycle time: 2, 3, 4 min

At least 20 patterns were produced for each combination of injection parameters, and they were measured 48 h after production using a Ferranti coordinate measuring machine (CMM), which has an accuracy level of 5 μm. The patterns were injected on a 12-tonne Temp Craft vertical-clamping-horizontal-injection manual injection press at a local investment casting company using temperature controlled platens. The wax used for injection was of water-emulsified type A7-TC2/E with a melting point range of 73–76°C.

It was found that the lower pressure values of 0.74 and 0.98 MPa did not produce acceptable patterns because there was insufficient pressure to achieve appropriate cavity filling. These low pressure levels were omitted from further trials. However, as will be discussed later, results at these values were still collected and analysed. It was also found that cavity filling improved as injection temperature increased. This is evident from the contraction chart of Fig. 5, where it is seen that the effect of pressure clearly starts from a pressure of 1.23 MPa at the 61°C injection temperature. The reason for this is that, as the temperature increased, the wax became less viscous and the injection pressure had less resistance to overcome. This produces better packing of material and results in reduced contraction. An optimal parameter range, that produced

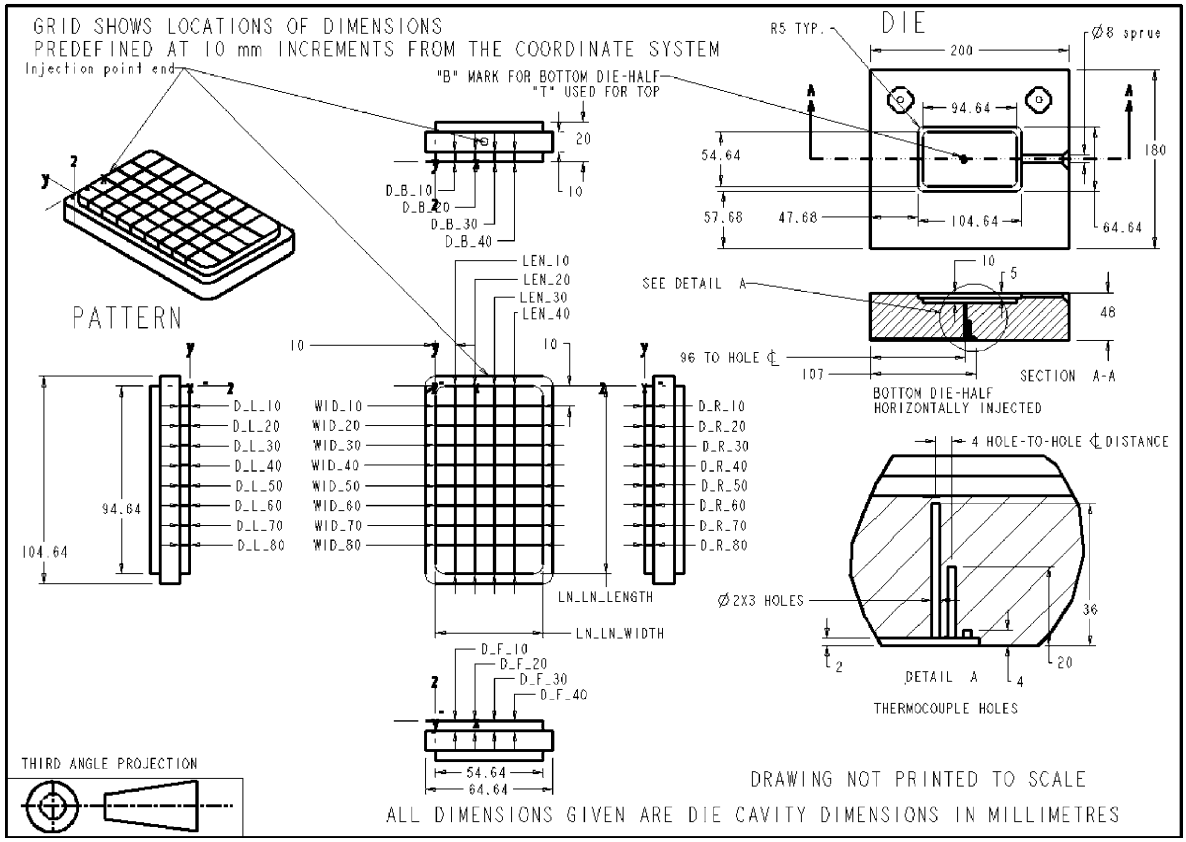

Fig. 4. Pattern and die geometry and dimensions.

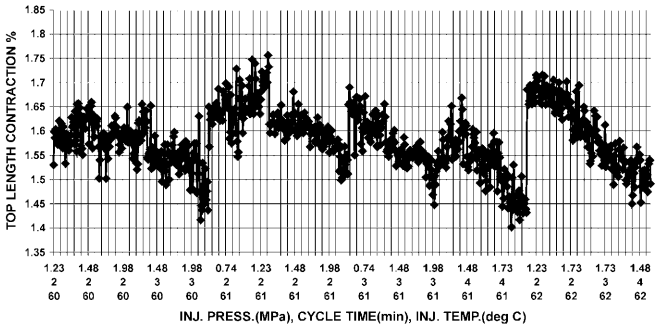

Fig. 5. Pattern topside length contraction (die = 94.639 mm).

patterns with good surface finish, was found to be at 61°C injection temperature, with a 1.23–1.98 MPa injection pressure and a 3 min cycle time. This was at the centre of the range used for the experimental trials conducted.

Normally, the wax pattern production room is temperature controlled and a steady temperature of about 22°C is usually maintained. This was verified by ambient temperature measurements taken during the experimental work. In the wax pattern room, two cooling processes take place. The first is usually rapid cooling in the temperature-controlled die. The second is a cooling process that takes place at a slower pace after ejection when the pattern cools at room conditions undergoing free contraction while it exchanges heat with the air mainly by free convection. Some injection presses, however, are equipped with a water cooling tank, in which the patterns fall immediately after ejection from the die. In this case, the after-ejection cooling rate is different. The patterns injected in the experiments described in this paper underwent free convection after ejection.

A number of pattern measurement points were defined and a program was developed for automatic measurement on the CMM. Corresponding points were measured on the die to minimise errors in the contraction calculations. The die was also marked to identify each die half. This mark was impressed onto each pattern so that the bottom and the top of the parts were treated and analysed separately. The pattern and die geometry with all designated dimensions are shown in Fig. 4. Every pattern was identified with a part number and appropriate records were made to match any pattern produced to the injection parameters, and to the corresponding die temperature profile it was produced under.

Die temperature profiles were also recorded for comparison with the temperature profiles of the heat transfer simulation. The results of the experiments were used to test the validity of the proposed model to predict wax pattern contraction.

5. Experimental Results and Discussion

Based on the observations of other parts injected with the same wax as was used in these experiments, it was found that, for an injection temperature of around 61°C, a final linear contraction value around 1.4% is usually reached. However, the results of these experiments show a shift in the contraction range. This can be seen in Fig. 5, where the mean contraction length is observed to be about 1.6%. This shift was partly due to inappropriate venting of the die, which resulted in some air being trapped in the patterns which increased the contraction on cooling.

Figure 5 also shows the results for one of the measured dimensions, i.e. the top length of the patterns. It can be seen that, initially, at the lowest injection temperature setting of 60°C, and the shortest cycle time of 2 min, the effect of injection pressure is not to decrease contraction, contrary to known trends. As the pressure increases to 1.48 MPa, the expected effect starts to appear and contraction decreases. However, as explained in Section 4, the 60°C injection temperature combined with the low injection pressures were found to be at the threshold of the start of packing for this component. This is more clearly seen at the injection temperature level of 61°C. As the pressure increases, a point is reached where any further pressure increase produced an almost linear decrease in contraction, and the trends are similar for the 62°C injection temperature setting. From this, it can be appreciated that for any component size and geometry, a point is reached where packing of extra material starts to occur, and therefore there are extra forces counteracting shrinkage at ejection time and during cooling to room temperature.

Because of the bulkiness of the component and relatively short cycle times used, it is noted that a considerable proportion of the mass of the pattern remained at a temperature close to injection temperature even at eject time. This can be seen in Fig. 6, which shows a pattern that has been cut open, just after ejection from the die, with the excess soft material removed. It also shows the actual solidified stable layer thickness of about 4 mm. Several patterns were opened during the experiments, and, in every case, it was observed that the bulk of the interior of the pattern was still soft in a state close to the congealing point of the wax. When all the soft material was removed, a consistent layer thickness of about 4–5 mm was evident. This solidified skin was not thick enough to withstand the forces of the material undergoing contraction internally and this meant that the whole of the pattern underwent free contraction on cooling to ambient. The net result was a shift in the otherwise expected contraction, but the effect was unchanged.

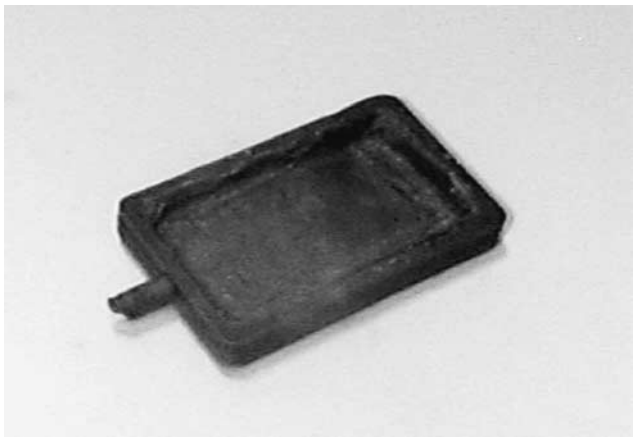

Fig. 6. Pattern cut open just after ejection.

Figure 7(*a*) shows the length contraction curve (i.e. contraction along the length of pattern), and Fig. 7 (*b*) shows the corresponding cooling curve of a pattern injected at 61°C, 2 min cycle time and 1.23 MPa injection pressure. The cooling curve shows temperature in °C against time of day in h (i.e. 15.00 means 3.00 p.m.). A thermocouple was inserted into the middle of the pattern just after ejection, and several length measurements were taken as the pattern cooled. On comparing the contraction curve with the cooling curve, it can be seen that the length decreased exponentially in the same fashion as the pattern internal temperature drops. It can also be observed from Fig. 7, that the majority of the contraction occurred within the first 2 h of cooling, after which both the contraction curve and the cooling curve have almost flattened out and the patterns have undergone about 95% of their total contraction. This result will be used to compare contractions against any model predictions.

Figure 8 shows a graph of the length contraction at ejection time. To obtain this data, every pattern injected in these experiments was measured immediately after ejection from the die using a vernier calliper with a 0.03 mm accuracy. This graph shows that, on average, the patterns have undergone about 30% of their total contraction at the time when they are ejected. This is a quantitative assessment of the amount of contraction that has taken place in the die, and will also be used to compare against modelling.

It was found that contraction occurred unequally in different directions. The length contraction parallel to injection flow was 1.6% on average; for width, perpendicular to flow it was 1.75%

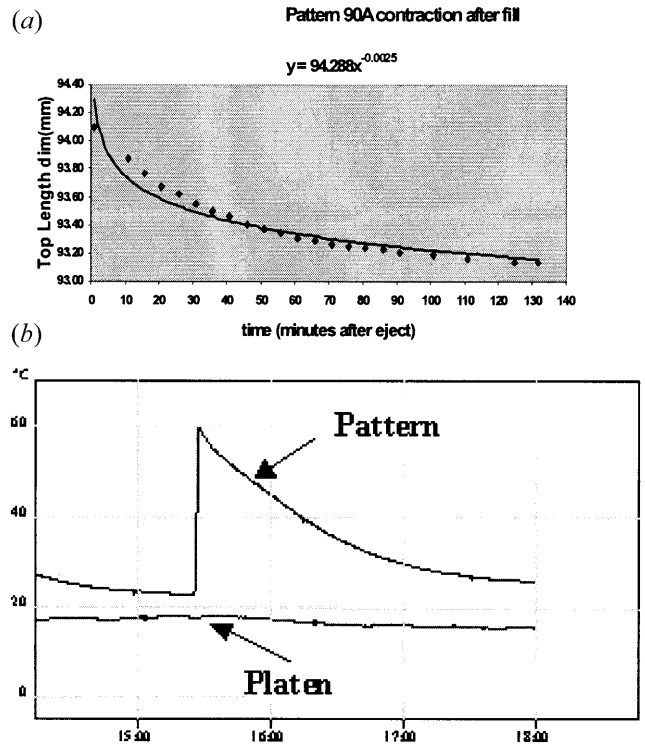

Fig. 7. Length contraction curve of a pattern injected at 61°C undergoing free contraction and corresponding cooling curves for the pattern and the platen.

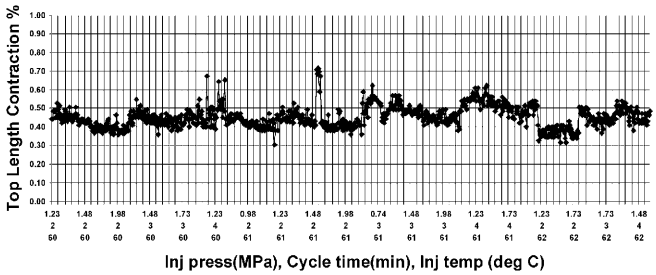

Fig. 8. Top length contraction just after ejection from the die.

on average and depth perpendicular to both flow and width was 2.6% on average. This is better seen in the local width contraction results of Fig. 9. This figure shows, for each pressure level, the width contraction of the pattern measured in a direction perpendicular to the filling flow direction at several distances from the injection point, as defined in Fig. 4.

Figure 9 shows at every pressure level, the local width contraction variation, which appears as an inverted "u" in shape in each case and in every case the local width distance from the gate increases from left to right. It can be seen that contraction decreases with increased pressure, and also that the width measurement closest to the injection point contracted slightly more than the width at the opposite end. This can be attributed to the temperature distribution because the closer the position was to the injection point, the longer it remained hot and the larger the contraction. In Fig. 9, it is also noted that the contraction is greatest at the mid-distance from the injection point. This can be attributed to factors such as the geometry of the component, which is quite bulky (i.e. 20 mm thick × 104.64 mm long × 64.64 mm wide). For the maximum cycle time used in this experiment of 4 min, there is still soft material in the middle of the pattern, and insufficient layer thickness at eject time. This allowed the shrinkage forces to overcome the strength of the lateral layers of the pattern and produced the distortion observed.

Figure 10 shows the local length contraction results with a similar effect. Again, at each pressure level, an inverted "u" shaped curve is observed, with the largest contraction at the mid-width point coincident with the injection point, where the support against deformation was the weakest. Contraction was found to be about the same as in Fig. 9 at equidistant length measurements from the injection point. The reverse effect is

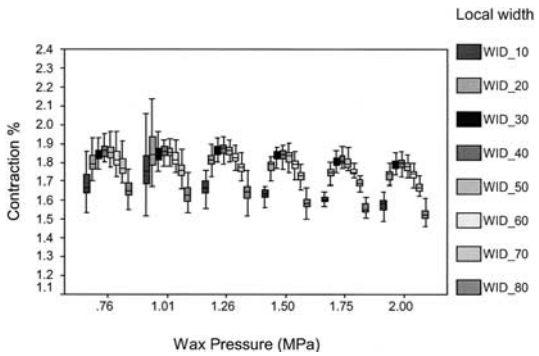

Fig. 9. Pattern local width contraction. Injection temperature = 61°C.

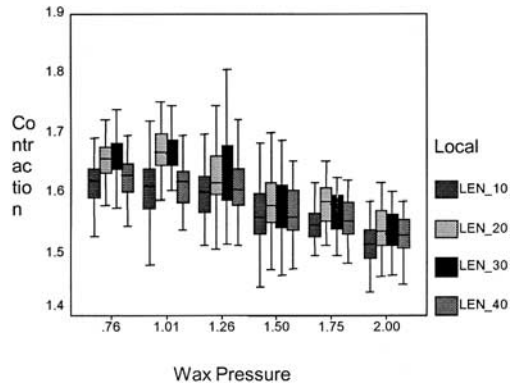

Fig. 10. Pattern local length contraction vs. injection pressure. Injection temperature = 61°C.

observed for the local depth contraction results as can be seen in Fig. 11, where each box in the "u" shaped curve at each pressure level represents a local depth measurement, whose distance from the gate decreases from left to right. Here, contraction was the greatest at the ends and smallest at the mid-length point. This indicates that the heat concentration effects dominated the pressure-packing effect at the recesses, especially at the corners, which remained hot longer and therefore contracted more. The local depth closest to the gate contracted slightly more than the local depth at the opposite end. This was in agreement with the observation of the local widths, and is attributable again to the injection end remaining hot longer than the opposite end.

6. Practical Applications of Results

Arising from the results of the current work some practical applications can be derived and are suggested as a guide for optimal injection parameter selection and for in-process control.

1. Based on the observations of experiments conducted, it was found that for the wax used, the pattern stable layer thickness at eject time was about 5 mm. From the numerical simulation graph of Fig. 3, the corresponding average temperature for an injection cycle of 3–4 min is about 47°C. DSC traces can be used to determine transformation fraction. This method is described in Speyer [7]. In the DSC trace of Fig. 1, the total cumulative area between the limits 60°C and 47°C is approximately 72.6 J g^{-1}. The 60°C mark represents the injection temperature and the 47°C mark represents the point at which full transformation from liquid to solid has occurred. Then, 72.6 J g^{-1} have to be removed in order to reduce the temperature from 60°C to 47°C. Therefore, the optimum cycle time can be determined for a required layer thickness and given part geometry and size and the die cooling load. Alternatively, the optimum die-cooling load for minimum cycle time can be determined.
2. Based on the results of the numerical simulations shown in Fig. 3, charts can be developed that show the interrelationships between pattern material and thickness, injection temperature, and die cooling load, to use as a guide in selecting an appropriate cycle time.
3. As shown in Fig. 7, most of the contraction occurs in the first two hours of cooling. This information can be used in process control. Given the pattern material and wax pattern production room ambient conditions, a pattern just ejected from the die can be measured and its temperature taken, and from the dimension obtained, an estimate can be made of the final dimension the pattern will reach. If the dimension is not on target, the injection parameters, whose effect on final dimensions is known, can be modified accordingly to compensate for the deviation and bring the process back on track.

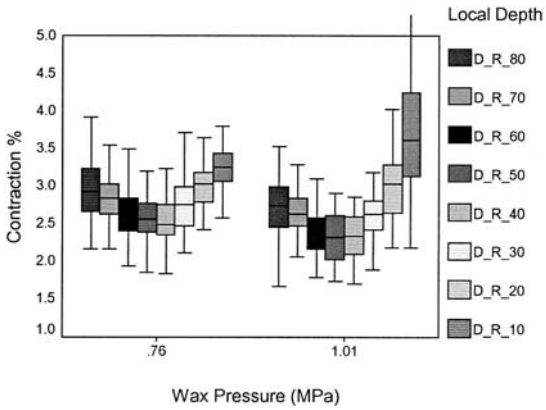

Fig. 11. Pattern local depth contraction vs. injection pressure. Injection temperature = 61°C.

7. Conclusions

The analytical tools needed to model the wax pattern contraction process have been identified and are currently being implemented. The results of the experiments were analysed and comparisons are made with the theoretical model. It has been found that to superimpose the effect of injection parameters on to the ideal contraction, the threshold of the start of that effect for the particular pattern geometry and size have to be known. Results indicate that computer-aided modelling can be used to predict the heat transfer occurring during the wax pattern contraction process and the ideal contraction, and the effects of injection parameters can then be added. The test case component has a null level of die constraint, and once this initial unconstrained model has been validated, further experiments must be conducted to incorporate the effects of constraint and different geometries. Future work will involve establishing and incorporating extra influencing factors and validating a full predictive model of final wax pattern contraction.

Acknowledgements

The authors wish to express their gratitude to the Cooperative Research Centre for Intelligent Manufacturing Systems and Technology (CRC for IMST) and A. W. Bell Ltd. (investment casting company), both in Melbourne, for their continuing support to this research program.

References

1. P. R. Beeley and R. F. Smart, Investment Casting, The Institute of Materials, Cambridge University Cambridge, UK, 1995.
2. Investment Casting Institute, Investment Casting Handbook 1980, ICI, USA, 154, 1980.
3. G. A. Bell, "Tooling", in P. R. Beeley and R. F. Smart (ed.), Investment Casting, The Institute of Materials. Cambridge University Press, UK, pp. 40–41, 1995.
4. M. Horacek, "Accuracy of castings manufactured by lost wax process", Proceedings of the 23rd British Investment Casting Trade Association Conference, Cambridge, UK, 2, pp. 1–20, 1997.
5. V. Okhuysen, K. Padmanaban and R. C. Voigt, "Tooling allowance practices in the investment casting industry", Proceedings of the 46th Annual Technical Meeting, Investment Casting Institute, Orlando, USA, pp. 1–25, 1998.
6. J. P. Holman, Heat Transfer, 8th edn, McGraw-Hill, NY, USA, pp. 168–170, 1997.
7. R. F. Speyer, Thermal Analysis of Materials, Marcel Dekker, NY, USA, p. 45, 1994.